Journal of Medicinal Chemistry

Article

Azepanone-Based Inhibitors of Human Cathepsin L

Robert W. Marquis, Ian James, Jin Zeng, Robert E. Lee Trout, Scott Thompson, Attiq Rahman, Dennis S. Yamashita, Ren Xie, Yu Ru, Catherine J. Gress, Simon Blake, Michael A. Lark, Shing-Mei Hwang, Thaddeus Tomaszek, Priscilla Offen, Martha S. Head, Maxwell D. Cummings, and Daniel F. Veber

J. Med. Chem., **2005**, 48 (22), 6870-6878• DOI: 10.1021/jm0502079 • Publication Date (Web): 30 September 2005

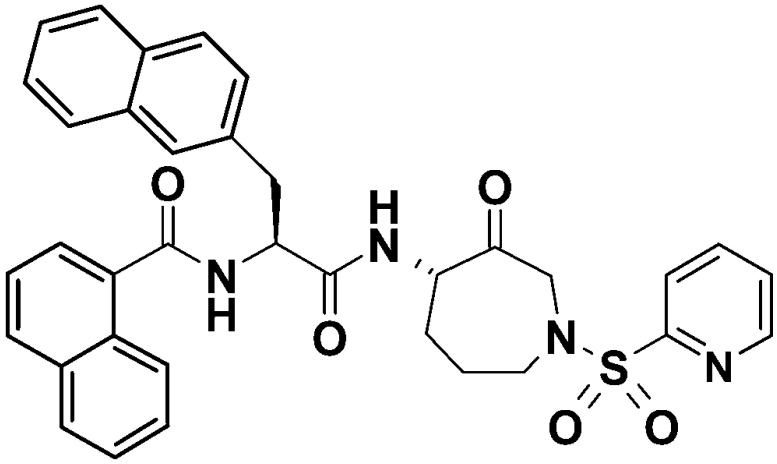

15

Cathepsin L K_i = 0.43 nM

Cathepsin K $K_{i,app}$ >10,000 nM

More About This Article

Additional resources and features associated with this article are available within the HTML version:

- Supporting Information
- Links to the 1 articles that cite this article, as of the time of this article download
- Access to high resolution figures
- Links to articles and content related to this article
- Copyright permission to reproduce figures and/or text from this article

Journal of Medicinal Chemistry is published by the American Chemical Society. 1155 Sixteenth Street N.W., Washington, DC 20036

Azepanone-Based Inhibitors of Human Cathepsin L

Robert W. Marquis,*,† Ian James,‡,§ Jin Zeng,† Robert E. Lee Trout,† Scott Thompson,† Attiq Rahman,† Dennis S. Yamashita,† Ren Xie,† Yu Ru,† Catherine J. Gress,‡,§ Simon Blake,‡,§ Michael A. Lark,‡,§ Shing-Mei Hwang,‡ Thaddeus Tomaszek,|| Priscilla Offen,⊥ Martha S. Head,⊥ Maxwell D. Cummings,⊥,# and Daniel F. Veber†,▽

Departments of Medicinal Chemistry, Bone and Cartilage Biology, Molecular Recognition, and Physical and Structural Chemistry, GlaxoSmithKline, 1250 South Collegeville Road, Collegeville, Pennsylvania 19426

Received March 7, 2005

The extension of a previously reported cathepsin K azepanone-based inhibitor template to the design and synthesis of potent and selective inhibitors of the homologous cysteine protease cathepsin L is detailed. Structure−activity studies examining the effect of inhibitor selectivity as a function of the P3 and P2 binding elements of the potent cathepsin K inhibitor **1** revealed that incorporation of either a P3 quinoline-8-carboxamide or a naphthylene-1-carboxamide led to increased selectivity for cathepsin L over cathepsin K. Substitution of the P2 leucine of **1** with either a phenylalanine or a β-naphthylalanine also resulted in an increased selectivity for cathepsin L over cathepsin K. Molecular modeling studies with the inhibitors docked within the active sites of both cathepsins L and K have rationalized the observed selectivities. Optimization of cathepsin L binding by the combination of the P3 naphthylene-1-carboxamide with the P2 β-naphthylalanine provided **15**, which is a potent, selective, and competitive inhibitor of human cathepsin L with a $K_i = 0.43$ nM.

Introduction

The recent completion of the sequencing of the human genome has revealed the encoding of 11 cysteine proteases of the papain superfamily.[1] One member of this family of cysteine proteases, cathepsin K, has been the subject of extensive studies reported from these and other laboratories.[2] Orally bioavailable azepanone-based inhibitors, which were designed to target this enzyme,[3] now appear to provide a general template for the inhibition of the papain family of cysteine proteases. Human cathepsin L (EC 3.4.22.15), an ubiquitously expressed lysosomal cysteine endopeptidase of this family,[4] has been implicated in a wide range of intra- and extracellular pathological and physiological processes including antigen presentation,[5] ovulation,[6] tumor growth and progression,[7] osteo and rheumatoid arthritis,[8] as well as bone resorption.[9] The cathepsin L knockout mouse (Ctsl −/−) displays a reduced antigen presentation, shedding of fur, and a reduction of trabecular bone volume.[10,11] Our interest in pursuing selective inhibitors of this enzyme is derived from the close homologies of cathepsins K and L as well as reports that have suggested that cathepsin L may play a role in the resorption phase of bone remodeling. Indeed, potent peptide aldehyde inhibitors of cathepsin L have been reported to attenuate bone resorption both in vitro and in the murine thyroparathroidectomized (TPTX) model of bone turnover.[12,13] Additionally, the bone-related phenotype in the cathepsin L knockout mouse suggests that potent and selective inhibitors of this protease may find utility in bringing further clarity to the exact role of this cysteine protease in bone resorption and other disparate pathological states.

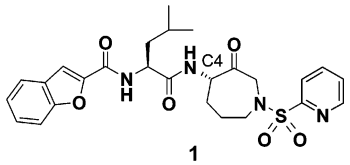

Figure 1.

A series of azepanone-based inhibitors of the osteoclast specific cysteine protease cathepsin K have been reported recently from these laboratories.[3] Azepanone **1** (Figure 1) was shown to be a potent inhibitor of cathepsin K in vitro as well as an inhibitor of bone resorption in cell-based assays. Analogue **1** has also been shown to be a potent inhibitor of Ca^{2+} release in the TPTX rat and to inhibit bone turnover in the ovariectomized monkey.[14] During the course of structure−activity studies to explore the effects of substitution of the P3 benzofuran-2-carboxamide and the P2 isobutyl groups of **1**, several potent and selective inhibitors of human cathepsin L were identified. In this paper, we disclose the optimization of both potency and selectivity of this azepanone class for the selective inhibition of cathepsin L. The studies reported in this account represent the first steps in a systematic, scaffold-based approach to the selective inhibition of individual members of the papain superfamily encoded by the human

* To whom correspondence should be addressed. Tel: 1-610-917-7368. Fax: 1-610-917-6020. E-mail: Robert.W.Marquis@gsk.com.
† Department of Medicinal Chemistry.
‡ Department of Bone and Cartilage Biology.
§ Current address: Centocor, 145 King of Prussia Rd., Radnor, PA 19087.
|| Department of Molecular Recognition.
⊥ Department of Physical and Structural Chemistry.
Current address: Johnson and Johnson Pharmaceutical Research and Development, L.L.C., 665 Stockton Drive, Exton, PA 19341.
▽ Current address: 290 Batleson Rd., Ambler, PA 19002.

10.1021/jm0502079 CCC: $30.25
Published on Web 09/30/2005

Scheme 1. Synthesis of Inhibitors **6**−**8**[a]

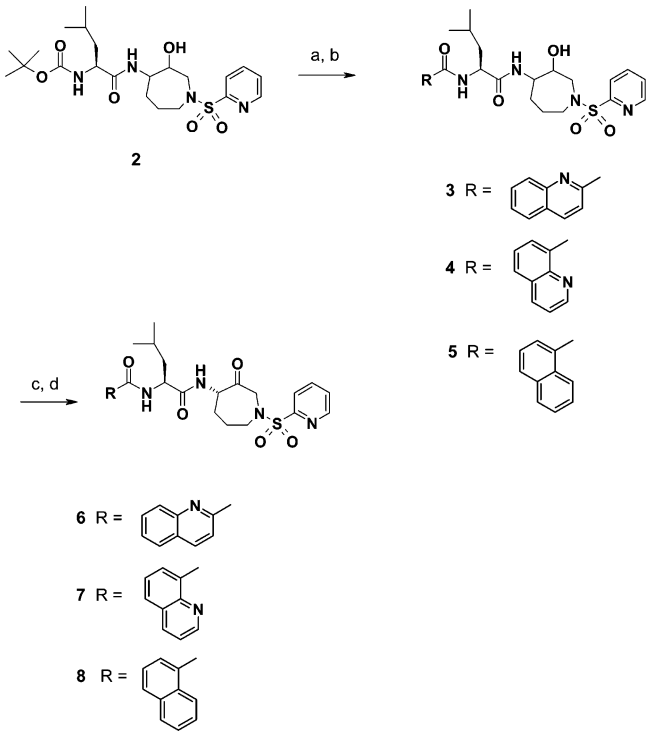

[a] Reagents and conditions: (a) 4 M HCl/dioxane, CH_3OH. (b) RCO_2H, EDC, HOBt, CH_2Cl_2. (c) Pyridine sulfur trioxide, TEA, DMSO or Dess−Martin periodinane. (d) HPLC separation.

Scheme 2. Synthesis of Inhibitors **13**−**15**[a]

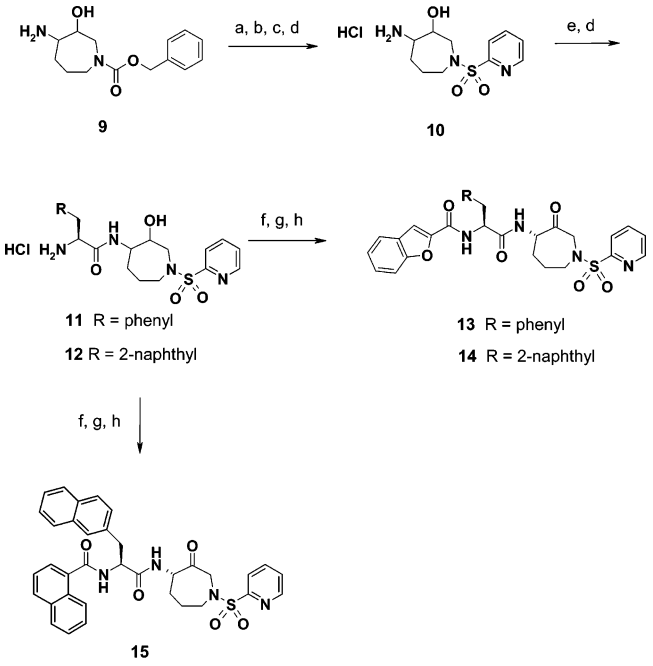

[a] Reagents and conditions: (a) Boc_2O, aqueous NaOH, 1,4-dioxane. (b) 10% Pd/C, H_2, CH_3OH. (c) 2-Pyridinesulfonyl chloride, $NaHCO_3$, CH_2Cl_2. (d) 4 M HCl/dioxane, CH_3OH. (e) N-Boc-phenylalanine or N-Boc-β-naphthylalanine, EDC, HOBt, CH_2Cl_2. (f) Benzofuran-2-carboxylic acid or 1-naphthoic acid, EDC, CH_2Cl_2. (g) Dess−Martin periodinane, CH_2Cl_2. (h) HPLC separation.

genome as well as those cysteine proteases implicated in diseases associated with parasitic infection.[15]

Synthesis Chemistry

The syntheses of inhibitors **6**−**8** began with sulfonamide **2**, the synthesis of which has been described previously (Scheme 1).[3] Treatment of **2** with 4 M HCl in dioxane followed by coupling of the resulting amine salt with either quinoline-2-carboxylic acid, quinoline-8-carboxylic acid, or naphthylene-1-carboxylic acid in the presence of EDC provided the intermediate alcohols **3**−**5** as mixtures of diastereomers. Oxidation of the alcohols **3**−**5** with either the Dess−Martin reagent or the pyridine sulfur trioxide complex followed by HPLC separation of the C-4 diastereomeric ketones provided inhibitors **6**−**8**. In the previously reported account of the synthesis and characterization of azepanone **1**, we had shown that the diastereomer that eluted first by HPLC was consistently the more potent inhibitor of cathepsin K. This observation was true for all members of the azepanone class of inhibitors. Azepanone **1**, the faster eluting and more potent of the C4 diastereomers, was shown by small molecule X-ray crystallography to possess the *S*-configuration at C-4. Additionally, an X-ray cocrystal structure of **1** bound within the active site of cathepsin K also confirmed the critical nature of the C-4 *S*-stereochemistry for effective binding. In these studies, the corresponding C-4 *R*-diastereomer was shown to possess at most 1/5000th the potency for cathepsin K than the C-4 *S*-diastereomer **1**. During the course of the work detailed in this manuscript, the same trend emerged whereby the slower eluting diastereomers were also significantly less active than their faster eluting counterparts. Because of this difference, the enzyme potencies of the slower eluting distereomers are not germane to the discussion presented herein. By analogy with our characterization of inhibitor **1**, we assume that the potent inhibitors described in this account possess the C-4 *S*-stereochemistry. We have also further confirmed this by the stepwise asymmetric synthesis of the C-4 *S*-diastereomer **15** (vida infra).

The syntheses of inhibitors **13**−**15** are outlined in Scheme 2. Protection of amino alcohol **9** with di-*tert*-butyl dicarbonate followed by hydrogenolysis of the carbonylbenzyloxy protecting group, sulfonylation of the resulting amine with 2-pyridylsulfonyl chloride, and removal of the *tert*-butoxycarbonyl protecting group under acidic conditions provided the amine salt **10**. Coupling of **10** with either N-Boc-phenylalanine or N-Boc-β-naphthylalanine and subsequent removal of the N-Boc protecting group gave intermediates **11** and **12**. Coupling of these amine salts with benzofuran-2-carboxylic acid in the presence of EDC followed by oxidation with the Dess−Martin reagent and separation of the C-4 diastereomers gave **13** and **14**. Alternatively, coupling of intermediate **12** with naphthlene-1-carboxylic acid followed by oxidation and HPLC separation of the diastereomeric ketones provided inhibitor **15**. Here again, the prevailing assumption is that the faster eluting, more potent diastereomer **15** possesses the C-4 *S*-stereochemistry. However, the somewhat equivocal nature of this critical stereochemical assignment was viewed as troublesome. In an effort to eliminate all ambiguities surrounding this issue, inhibitor **15** was synthesized utilizing the key chiral amino alcohol intermediate **17** (Scheme 3), which was synthesized in seven steps from oxazolidinone **16**.[16] Acylation of **17** with N-Boc-β-naphthylalanine in the presence of EDC followed by deprotection of the amine under acidic conditions provided the amine hydrochloride salt **18**.

Scheme 3. Enantiospecfic Synthesis of Inhibitor **15**[a]

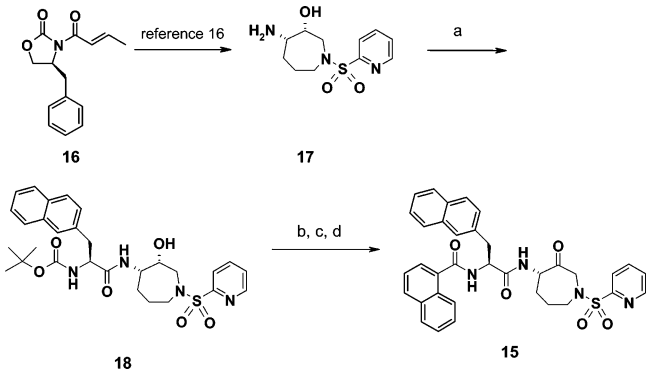

[a] Reagents and conditions: (a) N-Boc-β-naphthylalanine, EDC, HOBt, CH_2Cl_2. (b) 4 M HCl/dioxane, CH_3OH. (c) 1-Naphthoic acid, EDC, HOBt, CH_2Cl_2. (d) Dess−Martin periodinane, CH_2Cl_2.

Table 1. Cathepsins L, K, S, and B Inhibition Data[a]

	$K_{i,app}$ (nM)				
compd	Cat L	Cat K	Cat S	Cat B	ratio K/L
1	2.2	0.16	4.3	500	0.07
6	5.0	0.89	27	740	0.18
7	8.2	52	41	>1000	6.3
8	1.4	12	5.7		8.6
13	1.7	10.5	8.9	193	6.2
14	0.57	295	3.1	24	517
15	0.43	>10000	15.6	150	>20000

[a] $K_{i,app}$ values for all newly reported analogues represent the average of at least three independent titrations.

Acylation of **18** with 1-naphthoic acid followed by oxidation of the intermediate alcohol provided **15**, which was identical to the active C-4 *S*-diastereomer described above in Scheme 2. This chemical correlation provides further support for the critical role of the C-4 *S*-stereochemical assignment assumed in all of the inhibitors described in this account. From this work, we conclude that the stereochemical preference of the azepanone inhibitors described above for cathepsin L is identical to that seen for the previously reported inhibitors of cathepsin K.

Results and Discussion

Inhibitor Potencies and Selectivities. As has been shown previously, azepanone **1** is modestly selective for cathepsin K (K_i = 0.16 nM; Table 1) vs the highly homologous cathepsins L ($K_{i,app}$ = 2.2 nM; K/L = 0.07) and S ($K_{i,app}$ = 4.3 nM).[3] Not unexpectedly, **1** is very selective for cathepsin K over the cysteine exopeptidase cathepsin B ($K_{i,app}$ = 500 nM). In an in vitro cell-based assay of bone resorption, **1** is a potent inhibitor of native cathepsin K with an IC_{50} = 70 nM.[3,17] In an in situ cytochemical assay, a cell-based measure of cathepsin activity within human tissue sections containing osteoclasts, analogue **1** is also an effective inhibitor with an IC_{50} = 80 nM.[18] Upon the basis of the promising potency profile of **1**, an array-based approach was employed in order to probe the effect of substitution of the P3 benzofuran-2-carboxamide of **1** while retaining the invariant P2 isobutyl moiety. In a like manner, substitution of the P2 iso-butyl group of inhibitor **1** was probed while the P3 benzofuran-2-carboxamide remained constant. The results from these two independent studies have led to the identification of the potent and selective inhibitors of human cathepsin L reported in this account.

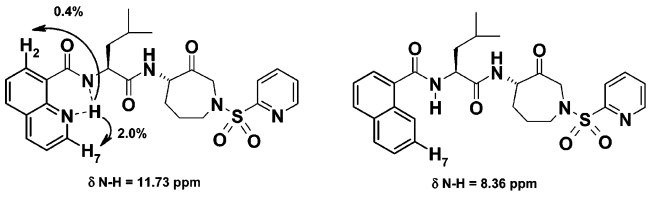

Figure 2. ^{1}H NMR spectroscopic data of inhibitors **7** and **8**.

Substitution of the P3 benzofuran-2-carboxamide of azepanone **1** with quinoline-2-carboxamide provided **6**, which is a potent inhibitor of cathepsin K with $K_{i,app}$ = 0.89 nM (Table 1). Relative to the benzofuran analogue **1**, incorporation of the P3 quinoline-2-carboxamide leading to **6** has led to a slight increase in selectivity over cathepsins L ($K_{i,app}$ = 5.0 nM; K/L = 0.18) and S ($K_{i,app}$ = 27 nM; S/L = 5.4). Substitution with the isomeric quinoline-8-carboxamide provided analogue **7**. Here, this P3 substitution has resulted in a significant reduction in potency versus cathepsin K ($K_{i,app}$ = 52 nM) relative to both **1** and **6** while maintaining potency for cathepsin L ($K_{i,app}$ = 8.2 nM; K/L = 6.3). Again, relative to azepanone **1**, the quinoline-8-carboxamide **7** shows improved selectivity vs cathepsins S and B with $K_{i,app}$ values of 41 and >1000 nM, respectively. Incorporation of the P3 naphthylene-1-carboxamide provided **8**, which is a potent inhibitor of cathepsin L ($K_{i,app}$ = 1.4 nM), approximately 8-fold selective over cathepsin K ($K_{i,app}$ = 12 nM). Interestingly, inhibitor **8**, which contains the P3 naphthylene-1-carboxamide, is more potent than corresponding P3 naphthylene-8-quinoline carboxamide derivative **7** in all of the enzymes examined (cat L $K_{i,app}$ = 1.4 nM; cat K $K_{i,app}$ = 12 nM; and cat S $K_{i,app}$ = 5.7 nM). An explanation for this difference in potencies was found upon inspection of the ^{1}H NMRs of both **7** and **8**. The ^{1}H NMR of the P3 quinoline-8-carboxamide analogue **7** (500 MHz, d_6-DMSO) shows a one proton doublet (J = 7.3 Hz) centered at 11.73 ppm corresponding to the N−H amide proton as indicated in Figure 2. Upon dilution, the chemical shift of this proton was unaltered. These data implicate the existence of an intramolecular hydrogen bond between the nitrogen of the quinoline-8-carboxamide moiety and the amide N−H as shown in Figure 2. This was further confirmed by a series of NOE difference experiments, which showed a 2% enhancement of the C-7 proton of the quinoline moiety upon irradiation of the N−H amide proton. A smaller enhancement (0.4%) was observed between the H-2 hydrogen of the quinoline and the N−H amide proton. The relative magnitude of these enhancements supports the presence of a significant degree of preorganization of the P3 quinoline-8-carboxamide of **7**.[19] Alternatively, the corresponding N−H proton of **8** is a one proton doublet (J = 7.3 Hz) centered at 8.36 ppm. The chemical shift of this proton relative to that contained within **7** suggests that it is not involved in a hydrogen-bonded interaction. Difference NOE experiments with **8** indicated that upon irradiation of the N−H proton there was no enhancement of the C-7 proton of the naphthyl moiety. Again, in combination,

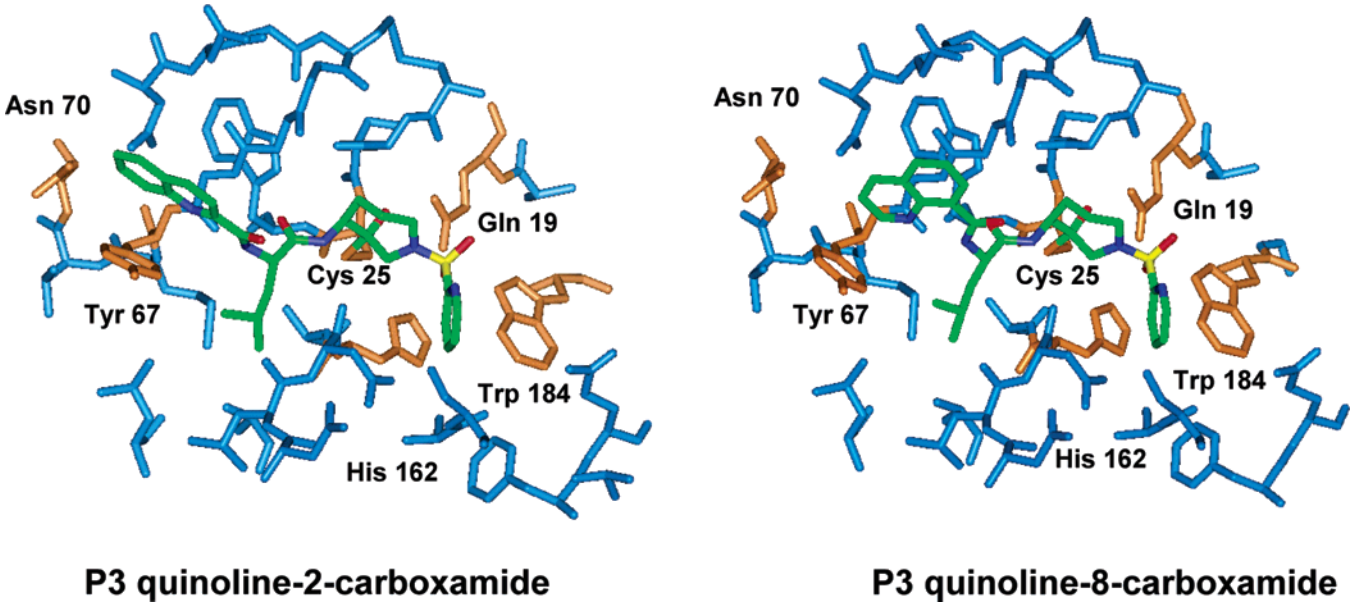

Figure 3. Docking of the P3 quinoline-2-carboxamide **6** and the quinoline-8-carboxamide **7** docked within the active site of human cathepsin K.

these data suggest that there is no intramolecular hydrogen bond within this portion of the molecule.

We conclude that the intramolecular hydrogen bond contained within **7** results in the reduced potency of this inhibitor on the cathepsins studied relative to that of analogue **8**. In the X-ray cocrystal structure of several pyrrolidinone[20] and azepanone-based inhibitors bound within the active site of cathepsin K, we have observed that this particular N−H of the inhibitors studied is involved in a critical hydrogen bond with the carbonyl oxygen of Gly 66 of the protein backbone.[21] To promote effective binding of **7** to cathepsins L, K, and S, the intramolecular hydrogen bond of the inhibitor must be disrupted, an energetically unfavorable process. As the Gly 66 residue is conserved throughout the papain superfamily of cysteine proteases, it is expected that there would be a concomitant reduction of inhibitor potency for all of these enzymes for inhibitor **7** relative to **8**. Indeed, this is reflected consistently in the $K_{i,app}$ values of inhibitors **7** and **8** versus all of the cysteine proteases examined in this study (Table 1).

In an effort to more fully understand the nature of the binding interactions of the P3 quinoline-8-carboxamide of **7**, which have led to the increased selectivity for cathepsin L relative to the P3 quinoline-2-carboxamide of **6**, a series of molecular modeling experiments were conducted. These studies utilized the previously published X-ray cocrystal structure of azepanone **1** bound within the active site of human cathepsin K (1NLJ, 2.0 Å)[3] and the X-ray crystal structure of human pro-cathepsin L (1CS8, 1.80 Å) from which the proregion had been deleted.[22] This modeled structure of human procathepsin L was utilized in the absence of an appropriate X-ray crystal structure of mature human cathepsin L. As seen in Figure 3, docking of **6** (cat K $K_{i,app} = 0.89$ nM; cat L $K_{i,app} = 5.0$ nM) within the active site of cathepsin K shows that the terminal aromatic group of the P3 quinoline-2-carboxamide is capable of maintaining a critical aromatic−aromatic interaction with Tyr 67 within the S3 pocket of the active site.[23] This interaction mimics the aromatic−aromatic interaction between the phenyl moiety of Tyr 67 of the protein backbone and the P3 benzofuran-2-carboxamide of the potent cathepsin K inhibitor **1** bound within the active site. Docking studies with inhibitor **7** (cat K $K_{i,app} = 52$ nM; cat L $K_{i,app} = 8.2$ nM) reveal that the aromatic−aromatic interaction between the Tyr 67 of cathepsin K and the quinoline-8-carboxamide moiety is partially eliminated. Rotation of quinoline-8-carboxamide group of **7** toward Tyr 67 creates a steric clash between these two moieties which would not promote an effective binding interaction. Alternatively, rotation of the quinoline-8-carboxamide away from Tyr 67 (not pictured) in order to alleviate this poor interaction leads to unfavorable steric interactions with Asp 61 and Gly 64 of the protein backbone. This poor interaction between the P3 quinoline-8- carboxamide of **7** and the Tyr 67 coupled with the steric crowding of the inhibitor with Asp 61 and Gly 64 represents what is believed to be a plausible explanation for the reduced potency of this compound for cathepsin K.

A comparison of the X-ray crystal structures as well as the primary amino acid sequences of cathepsins K and L reveal two critical differences in amino acid residues within the S3 binding pockets of these enzymes that may account for the similar cathepsin L potencies of **1**, **6**, and **7**. The first of these differences is that Tyr 67 in the S3 binding pocket of cathepsin K is replaced by Leu 69 in cathepsin L (see Figures 4 and 5). The presence of the hydrophobic Leu 69 residue in cathepsin L would eliminate the possibility of an aromatic−aromatic interaction within the S3 pocket of this enzyme. This was seen to be a key interaction in the docking studies and in the X-ray cocrystal structure of **1** bound in the active site of cathepsin K. Second, a comparison of the aromatic residues within the S3 binding pockets of cathepsins K and L shows that the aromatic group within the S3 pocket of cathepsin L is Tyr 72 which is located at the end of this pocket. As discussed above, the aromatic residue in the S3 binding pocket of cathepsin K is Tyr 67 which is located at the bottom of this hydrophobic pocket (compare Figures

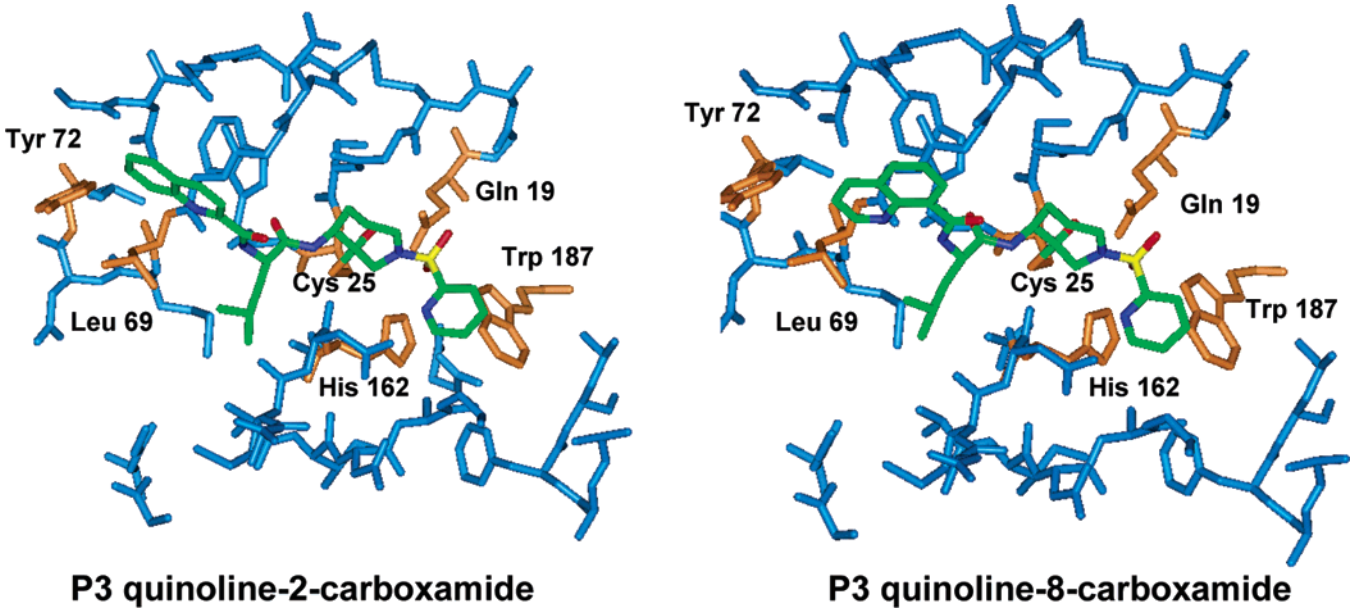

Figure 4. Docking of the P3 quinoline-2-carboxamide **6** and the quinoline-8-carboxamide **7** docked within the active site of human procathepsin L (for clarity, the proregion has been deleted).

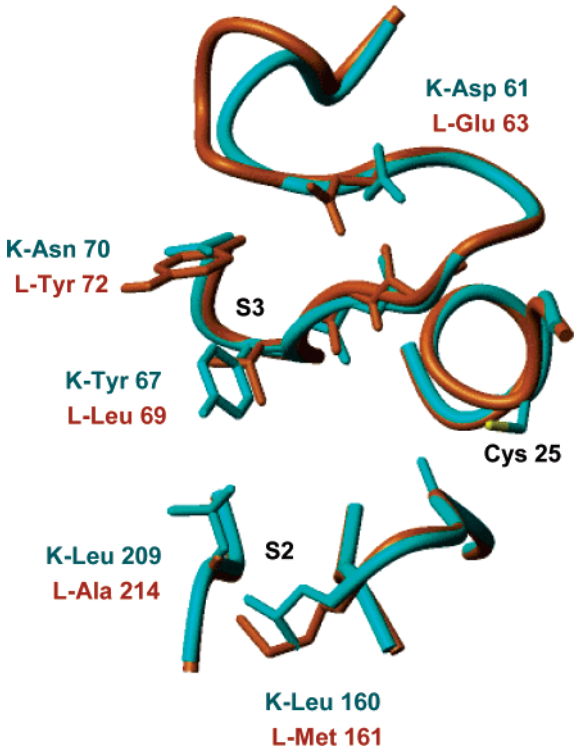

Figure 5. Overlay of the P3 and P2 binding pockets within the active sites of cathepsin L (orange) and cathepsin K (aqua) highlighting the residues within these pockets that are critical in determining the specificities for these cysteine proteases.

3−5). The relative locations of the aromatic amino acid residues present in the S3 binding pockets of cathepsins L and K suggest that cathepsin L may be less sensitive to the differences between the P3 aromatic moieties of inhibitors **1**, **6**, and **7**. The similar cathepsin L potencies of these azepanones suggest this to be true (Table 1). Docking of **6** and **7** within the active site of cathepsin L (Figure 4) shows that the quinoline-2-carboxamide of **6** may be capable of a ring−ring interaction with Tyr 72 of cathepsin L. The conformation required for the binding of the quinoline-8-carboxamide of **7** could not engage Tyr 72 in a similar interaction. However, in this instance, the P3 quinoline-8-carboxamide moiety may be able to remain buried within the S3 pocket since the iso-butyl side chain of Leu 69 is smaller and should possess the appropriate conformational flexibility to permit the binding of this group.

Investigation of the effect of the substitution of the P2 iso-butyl moiety of **1** on inhibitor selectivities revealed that azepanone **13**, which incorporates a P2 benzyl group, was 6-fold more selective for cathepsin L over cathepsin K (cat K $K_{i,app}$ = 10.2 nM; cat L $K_{i,app}$ = 1.7 nM), 5-fold selective over cathepsin S ($K_{i,app}$ = 8.9 nM), and 113-fold selective over cathepsin B ($K_{i,app}$ = 193 nM). Extension of the P2 aromatic group via the incorporation of the P2 β-naphthylalanine to provide **14** further increased selectivity for cathepsin L via a diminution in potency for cathepsin K (cat K $K_{i,app}$ = 290 nM; cat L $K_{i,app}$ = 0.57 nM; cat K/L = 517). The potency of **14** for the inhibition of cathepsin S ($K_{i,app}$ = 3.1 nM) was similar to that of inhibitor **13**. The potency of **14** for the inhibition of cathepsin B ($K_{i,app}$ = 42 nM) increased 7-fold relative to the P2 phenylalanine analogue **13**.

Brömme and co-workers have investigated the effect that substitution of the P2 amino acid residue plays in determining selectivities of cathepsins K, L, and S on rate ratios for a series of irreversible vinyl sulfone inhibitors.[24] These studies and others have shown that the hydrophobic S2 binding pocket of cathepsin K is specific for leucine.[25] On the basis of this work as well as modeling studies, the loss in potency for cathepsin K upon incorporation of the P2-benzyl or naphthyl moieties is likely the result of a steric clash of these groups with Leu 160 and/or Leu 209 within the S2 pocket of the active site. These residues serve to effectively limit access of larger amino acid residues (Figure 5) into the S2 binding pocket. The corresponding residues of the S2 pocket of cathepsin L are Ala 214 and Met 161. Here, the smaller alanine side chain in combination with the conformationally more flexible Met 161 make the S2 pocket of cathepsin L larger and

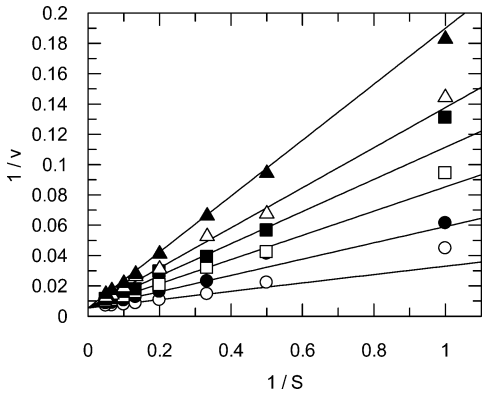

Figure 6. Lineweaver−Burk plot of inhibitor **15**.

permit access of the phenyl and naphthyl moieties of inhibitors **13** and **14**.

From the above-mentioned structure−activity relationship and modeling studies, azepanones **8** and **14** were identified as possessing individually the optimal binding elements required for the P2 and P3 pockets of human cathepsin L. A combination of the naphthylene-1-carboxamide of **8** with the P2 of the β-naphthylalanine of **14** has led to azepanone **15**, which is a 0.43 nM inhibitor of cathepsin L with greater than 20000-fold selectivity over cathepsin K ($K_{i,app}$ = >10000 nM). It is 36-fold selective for cathepsin L over cathepsin S ($K_{i,app}$ = 15.6 nM) and 340-fold selective over cathepsin B ($K_{i,app}$ = 150 nM). The Lineweaver−Burk plot (Figure 6) showed a constant 1/v axis intercept with increasing substrate concentrations, indicative of a competitive mode of inhibition of cathepsin L by **15**.

As reported previously, inhibitor **15** was devoid of activity in the in situ cyctochemical assay when evaluated at concentrations up to 1 μM and was also inactive in an in vitro assay of bone resorption, which employs osteoclasts harvested from osteoclastomas up to a concentration of 300 nM.[3,26,27] In contrast, inhibitor **1** (cathepsin K_i = 0.16 nM) has been reported to be a potent inhibitor in both the in situ cytochemical assay (IC_{50} = 70 nM) and the human osteoclast resorption assay (IC_{50} = 80 nM). These results have suggested that it is the inhibition of the latter enzyme that is required for the attenuation of bone resorption by small molecule inhibitors rather than the inhibition of cathepsin L.

It is also now recognized that the previously reported selective peptide-derived aldehyde inhibitors of cathepsin L, which, in part, formed the basis for the hypothesis of this protease's importance in bone resorption, are in actuality at least as potent inhibitors of human cathepsin K, a property not explored in these earlier studies.[28]

Conclusions

In this paper, we have detailed the extension of the azepanone template of cathepsin K inhibitors to the design and synthesis of potent and selective inhibitors of the highly homologous cysteine protease cathepsin L. Structure−activity studies investigating substitution of the P3 benzofuran-2-carboxamide of the potent cathepsin K inhibitor **1** led to the discovery that incorporation of a P3 quinoline-8-carboxamide or naphthylene-1-carboxamide resulted in a diminution of cathepsin K inhibition while retaining potent cathepsin L activity. Molecular modeling experiments were able to account for the increased cathepsin L/K selectivity suggesting that the quinoline-8-carboxamide and, by extension, the closely related naphthylene-1-carboxamide, cannot effectively engage Tyr 67 within the S3 pocket of cathepsin K in a critical aromatic−aromatic interaction. Additionally, the incorporation of the P3 quinoline-8-carboxamide was shown to result in a steric clash with amino acid residues Asp 61 and Gly 64 within this same binding pocket. Replacement of the P2 leucine moiety of azepanone **1** with either a phenylalanine or a β-naphthylalanine also resulted in a loss of potency vs cathepsin K while retaining potencies for both cathepsins L and S. This increase in cathepsin L and S selectivity vs cathepsin K was related to the inability of the smaller more restrictive S2 binding pocket of cathepsin K to accommodate the larger phenyl or naphthyl moieties. Both cathepsins L and S, which possess larger S2 binding pockets, permitted the binding of these aromatic groups.

These potent and selective inhibitors should play a useful role in helping to further define the role of cathepsin L in both normal and pathological physiology. Through the incorporation of the appropriate P3, P2, and P1′ specificity determinants, we anticipate that this azepanone template may be extended to the selective inhibition of many members of the papain family of cysteine proteases.

Experimental Section

General. Materials and reagents were used as supplied. Nuclear magnetic resonance spectra were recorded at either 250, 400, or 500 MHz. Mass spectra were taken on a PE Syx API III instrument using electrospray (ES) ionization techniques. Elemental analyses were obtained using a Perkin-Elmer 240C elemental analyzer. Reactions were monitored by TLC analysis using Analtech Silica Gel GF or E. Merck Silica Gel 60 F-254 thin layer plates. Flash chromatography was carried out on E. Merck Kieselgel 60 (230−400 mesh) silica gel.

Quinoline-2-carboxylic Acid {(*S*)-1-[3-Oxo-1-(pyridine-2-sulfonyl)azepan-4-ylcarbamoyl]-3-methyl-butyl}-amide (6). To a solution of **2** (1.20 g, 2.48 mmol) in CH_3OH (5.0 mL) was added 4 M HCl in dioxane (5 mL). This mixture was maintained at room temperature for approximately 2 h whereupon it was concentrated to provide 1.1 g of (*S*)-2-amino-4-methyl-pentanoic acid [3-hydroxy-1-(pyridine-2-sulfonyl)-azepan-4-yl]amide hydrochloride as a white powder, which was used in the following step with no further purification. To a solution of the amine hydrochloride (0.57 g, 1.25 mmol) in CH_2Cl_2 (10 mL) were added TEA (0.44 mL, 3.12 mmol), EDC (0.26 g, 1.38 mmol), HOBt (0.17 g, 1.25 mmol), and quinoline-2-carboxylic acid (0.22 g, 1.25 mmol). This mixture was maintained at room temperature until complete consumption of the starting material was observed as determined by TLC analysis. The mixture was concentrated, and the residue was dissolved in EtOAc and washed with saturated $NaHCO_3$ and brine. The organic layer was dried ($MgSO_4$), filtered, and concentrated. Column chromatography (4:1 EtOAc:hexanes) of the residue provided 0.67 g (64%) of **3** as a white powder. ^{1}H NMR (400 MHz, $CDCl_3$): δ 8.74−8.52 (m, 2H), 8.36 (m, 2H), 8.22 (m, 1H), 8.05−7.51 (m, 5H), 6.72 (m, 1H), 4.63 (m, 1H), 4.15 (m, 1H), 4.05−3.24 (m, 6H), 2.03−1.65 (m, 8H), 1.07 (m, 6H). MS (ESI) 540.4 $(M + H)^+$. To a solution of alcohol **3** (0.36 g, 0.67 mmol) in DMSO (2.0 mL) were added TEA (0.93 mL, 6.68 mmol) and pyridine sulfur trioxide complex (0.53 g, 3.34 mmol). This mixture was maintained at room temperature for approximately 2 h whereupon it was diluted with EtOAc and washed with saturated $NaHCO_3$ and brine, dried ($MgSO_4$), filtered, and concentrated. Column chromatography (2:1 EtOAc:hexanes) provided 0.29 g (81%) of the diastereomeric mixture as

a white powder. Separation of this mixture by preparative HPLC (50:50 hexanes:ethanol, 10 μ 100 Å (R,R) Whelk-O, 25 cm × 21.1 mm ID) gave 0.07 g of the desired faster eluting *S*-diastereomer. ^{1}H NMR (400 MHz, $CDCl_3$): δ 8.72 (d, J = 8.22 Hz, 1H), 8.68 (d, J = 4.76 Hz, 1H), 8.34 (d, J = 8.46 Hz, 1H), 8.30 (d, J = 8.46 Hz, 1H), 8.22 (d, J = 8.53 Hz, 1H), 7.96 (d, J = 7.68 Hz, 1H), 7.93 (td, J = 7.74, 1.60 Hz, 1H), 7.89 (d, J = 8.20 Hz, 1H), 7.79 (t, J = 7.67 Hz, 1H), 7.64 (t, J = 7.49 Hz, 1H), 7.51 (m, 1H), 7.13 (d, J = 6.38 Hz, 1H), 5.12 (m, 1H), 4.75 (d, J = 19.8 Hz, 1H), 4.72 (m, 1H), 4.09 (d, J = 14.7 Hz, 1H), 3.80 (d, J = 19.0 Hz, 1H), 2.65 (t, J = 12.5 Hz, 1H), 2.22 (m, 1H), 2.12 (m, 1H), 1.80 (m, 4H), 1.43 (m, 1H), 1.01 (d, J = 4.41 Hz, 3H), 0.99 (d, J = 4.28 Hz, 3H). ^{13}C NMR (125.77 MHz, $CDCl_3$): δ 205.8, 170.9, 164.2, 157.2, 150.2, 148.8, 146.1, 138.2, 137.9, 130.4, 129.6, 129.4, 128.2, 127.7, 127.0, 122.4, 119.0, 58.7, 57.9, 52.1, 51.3, 41.3, 31.7, 28.3, 24.9, 22.9, 22.1. MS (ES) 538.2 $(M + H)^+$. Elemental analysis ($C_{27}H_{31}N_5O_5S$) C, H, N.

Quinoline-8-carboxylic Acid {(*S*)-1-[3-Oxo-1-(pyridine-2-sulfonyl)azepan-4-ylcarbamoyl]-3-methyl-butyl}-amide (7). ^{1}H NMR (500 MHz, $CDCl_3$): δ 11.72 (d, 1H), 8.97 (dd, 1H), 8.86 (dd, 1H), 8.70 (d, 1H), 8.29 (dd, 1H), 7.95−7.92 (m, 3H), 7.69 (t, 1H), 7.53−7.51 (m, 2H), 7.34 (d, 1H), 5.13 (m, 1H), 4.81 (q, 1H), 4.73, d, 1H), 4.14 (d, 1H), 3.79 (d, 1H), 2.67 (dt, 1H), 2.23 (dd, 1H), 2.18−2.08 (m, 1H), 1.91−1.81 (m, 4H), 1.43 (m, 1H), 1.01 (dd, 6H). ^{13}C NMR (62.9 MHz, d_6-DMSO): 205.73, 171.7, 166.1, 157.3, 150.2, 149.5, 145.6, 138.1, 137.7, 134.1, 132.2, 128.5, 128.1, 126.9, 126.5, 122.4, 121.0, 58.6, 57.8, 52.7, 51.3, 40.7, 31.7, 28.3, 25.1, 23.1, 22.1. MS (ESI) 538.2 $(M + H)^+$. Elemental analysis ($C_{27}H_{31}N_5O_5S$) C, H, N.

Naphthoic-1-carboxylic Acid {(*S*)-1-[3-Oxo-1-(pyridine-2-sulfonyl)azepan-4-ylcarbamoyl]-3-methyl-butyl}-amide (8). ^{1}H NMR (500 MHz, d_6-DMSO): δ 8.76 (d, 1H), 8.66 (d, 1H), 8.23 (1H, d), 8.22 (d, 1H), 8.12 (dd, 1H), 8.02 (m, 3H), 7.74 (ddd, 1H), 7.56 (m, 4H), 4.86 (m, 1H), 4.63 (m, 1H), 4.43 (d, 1H), 3.86 (d, 2H), 2.87 (m, 1H), 1.86−1.80 (m, 3H), 1.66 (m, 1H), 1.63−1.57 (m, 3H), 0.96 (d, 3H), 0.92 (d, 3H). ^{13}C NMR (62.9 MHz, d_6-DMSO): 205.56, 171.66, 168.62, 156.25, 150.47, 139.08, 134.58, 133.07, 129.76, 128.14, 127.62, 126.69, 126.21, 125.44, 125.30, 124.95, 122.17, 57.84, 57.21, 51.48, 50.13, 40.29, 39.99, 39.83, 39.66, 39.33, 39.16, 38.99, 29.77, 28.34, 24.48, 23.18, 21.36. MS (ESI) 540.2 $(M + H)^+$.

Benzofuran-2-carboxylic Acid {(*S*)-1-[3-Oxo-1-(pyridine-2-sulfonyl)azepan-4-ylcarbamoyl]-2-phenyl-ethyl}-amide (13). To a solution of **10** (1.5 g, 4.88 mmol) in CH_2Cl_2 (25 mL) were added N-Boc phenylalanine (1.30 g, 4.88 mmol), EDC (1.03 g, 5.37 mmol), HOBt (0.66 g, 4.88 g), and TEA (1.7 mL, 12.2 mmol). This mixture was maintained at room temperature until complete consumption of the starting material was observed whereupon it was concentrated. The residue was diluted with EtOAc and washed with saturated $NaHCO_3$ and brine. The organic layer was dried ($MgSO_4$), filtered, and concentrated. Column chromatography (4:1 EtOAc:hexanes) of the residue provided 1.47 g (58%) of {(*S*)-1-[3-hydroxy-1-(pyridine-1-sulfonyl)azepan-4-ylcarbamoyl]-2-phenyl-ethyl}-carbamic acid *tert*-butyl ester as a white powder. MS (ESI) 519.2 $(M + H)^+$. To a solution of {(*S*)-1-[3-hydroxy-1-(pyridine-1-sulfonyl)azepan-4-ylcarbamoyl]-2-phenyl-ethyl}carbamic acid *tert*-butyl ester (1.2 g, 2.32 mmol) in methanol (23 mL) was added a solution of 4 M HCl in dioxane (5.8 mL). This mixture was maintained at room temperature overnight whereupon it was concentrated and azeotropically dried with toluene (3×) to provide 1.12 g of **11** as a white powder, which was used in the following step with no further purification. MS (ESI) 419.4 $(M + H)^+$. To a mixture of **11** (0.20 g, 0.44 mmol), 2-benzofurancarboxylic acid (0.077 g, 0.48 mmol), EDC (0.095 g, 0.50 mmol), and HOBt (0.067 g, 0.50 mmol) were added CH_2Cl_2 (4.5 mL) and TEA (0.25 mL, 1.8 mmol). The reaction mixture was stirred under argon at room temperature for 22 h. The reaction was diluted with ethyl acetate and washed successively with saturated K_2CO_3 and brine. The combined aqueous layers were then back extracted with ethyl acetate. The combined organic layers were dried over $MgSO_4$, filtered, and concentrated. Column chromatography (4% CH_3OH:CH_2Cl_2) yielded 0.17 g (68%) of the intermediate alcohol as a white powder. ^{1}H NMR (400 MHz, $CDCl_3$, as a mixture of diastereomers): δ 8.71 (m, 1H), 7.95 (m, 2H), 7.68 (m, 1H), 7.51−7.42 (m, 4H), 7.32−7.26 (m, 6H), 6.54 (m, 1H), 4.89 (m, 1H), 3.77−3.59 (m, 3H), 3.41 (m, 2H), 3.30−3.20 (m, 3H), 1.84 (m, 4H), 1.67 (m, 2H). MS (ESI) 563.0 $(M + H)^+$. To a solution of the diastereomeric alcohols (0.33 g, 0.59 mmol) in CH_2Cl_2 (6.0 mL) was added Dess−Martin periodinane (0.37 g, 0.88 mmol). The reaction was stirred under argon at room temperature for 1.5 h whereupon it was diluted with CH_2Cl_2 and washed with 10% aqueous $Na_2S_2O_3$ and two portions of saturated $NaHCO_3$, dried (Na_2SO_4), filtered, and concentrated. Column chromatography (1:2 hexanes:ethyl acetate) followed by preparative HPLC (50:50 hexanes:ethanol, 10 μ 100 Å (R,R) Whelk-O, 25 cm × 21.1 mm ID) provided 0.074 g of the desired ketone **13** (22.5%) as a white powder. ^{1}H NMR (400 MHz, $CDCl_3$): δ 8.67 (d, J = 4.74 Hz, 1H), 7.96 (d, J = 7.79 Hz, 1H), 7.92 (td, J = 7.63, 1.46 Hz, 1H), 7.66 (d, J = 7.77 Hz, 1H), 7.52 (m, 2H), 7.46 (s, 1H), 7.43 (t, J = 7.25 Hz, 1H), 7.35−7.22 (m, 7H), 6.54 (d, J = 5.89 Hz, 1H), 5.00 (m, 1H), 4.84 (dd, J = 14.2, 8.06 Hz, 1H), 4.68 (dd, J = 19.1, 1.30 Hz, 1H), 4.09 (d, J = 15.0 Hz, 1H), 3.73 (d, J = 19.0 Hz, 1H), 3.27 (dd, J = 13.5, 6.05 Hz, 1H), 3.08 (dd, J = 13.5, 8.36 Hz, 1H), 2.62 (t, J = 12.6 Hz, 1H), 2.18 (m, 2H), 1.81 (m, 1H), 1.31 (m, 1H). ^{13}C NMR (125.77 MHz, $CDCl_3$): δ 205.0, 169.5, 158.4, 157.2, 154.8, 150.2, 148.1, 138.2, 136.1, 129.2, 128.9, 127.5, 127.3, 127.1, 127.0, 123.7, 122.7, 122.4, 112.0, 110.9, 58.5, 57.9, 54.6, 51.3, 39.2, 31.7, 28.3. MS (ESI) 561.0 $(M + H)^+$.

Benzofuran-2-carboxylic Acid {(*S*)-1-[3-Oxo-1-(pyridine-2-sulfonyl)azepan-4-ylcarbamoyl]-2-naphthylen-2-yl}amide (14). ^{1}H NMR (400 MHz, $CDCl_3$): δ 8.66 (d, J = 4.43 Hz, 1H), 7.97 (d, J = 7.75 Hz, 1H), 7.92 (td, J = 7.68, 1.39 Hz, 1H), 7.82 (m, 3H), 7.71 (s, 1H), 7.66 (d, J = 7.76 Hz, 1H), 7.54−7.36 (m, 8H), 7.28 (t, J = 7.53 Hz, 1H), 6.53 (d, J = 5.99 Hz, 1H), 5.04 (m, 1H), 4.92 (dd, J = 14.0, 8.03 Hz, 1H), 4.47 (d, J = 18.4 Hz, 1H), 4.06 (d, J = 15.0 Hz, 1H), 3.62 (d, J = 19.0 Hz, 1H), 3.44 (dd, J = 13.5, 5.84 Hz, 1H), 3.23 (dd, J = 13.5, 8.32 Hz, 1H), 2.56 (t, J = 12.5 Hz, 1H), 2.12 (m, 2H), 1.78 (m, 1H), 1.29 (m, 1H). ^{13}C NMR (125.77 MHz, $CDCl_3$): δ 204.8, 169.5, 158.4, 157.2, 154.8, 150.2, 148.1, 138.2, 133.6, 133.5, 132.6, 128.7, 128.0, 127.6, 127.5, 127.2, 127.1, 127.0, 126.3, 125.8, 123.7, 122.7, 122.5, 112.0, 111.0, 58.4, 57.8, 54.6, 51.2, 39.3, 31.7, 28.2. MS (ESI) 611.2 $(M + H)^+$.

Naphthalene-2-carboxylic Acid {(*S*)-2-Naphthalen-2-yl-1-[(*S*)-3-oxo-1-(pyridine-2-sulfonyl)azepan-4-ylcarbamoyl]ethyl}amide (15). To a mixture of the amine hydrochloride **12** (0.51 g, 1.0 mmol), 1-naphthoic acid (0.18 g, 1.0 mmol), EDC (0.21 g, 1.1 mmol), and HOBt (0.15 g, 1.1 mmol) were added CH_2Cl_2 (10 mL) and TEA (0.56 mL, 4.0 mmol). The mixture was maintained under argon at room temperature for 18 h whereupon it was diluted with ethyl acetate and washed with saturated K_2CO_3 and brine. The combined aqueous layers were then back extracted with ethyl acetate. The combined organic layers were dried over $MgSO_4$, filtered, and concentrated. Column chromatography (4% CH_3OH:CH_2Cl_2) yielded 0.42 g (67%) of the diastereomeric alcohols as a white powder. ^{1}H NMR (400 MHz, $CDCl_3$, as a mixture of diastereomers): δ 8.66 (m, 1H), 7.95−7.79 (m, 9H), 7.47 (m, 6H), 7.35 (m, 1H), 7.23 (m, 1H), 6.82 (m, 1H), 5.18 (m, 1H), 3.79 (m, 1H), 3.62 (m, 1H), 3.51−3.26 (m, 5H), 1.70 (m, 4H), 1.58−1.42 (m, 3H). MS (ESI) 623.0 $(M + H)^+$. To a solution of the alcohols (0.41 g, 0.66 mmol) in CH_2Cl_2 (6.5 mL) was added Dess−Martin periodinane (0.45 g, 1.0 mmol). The reaction was maintained under argon at room temperature for 1.5 h whereupon it was diluted with CH_2Cl_2 and washed with 10% aqueous $Na_2S_2O_3$ and two portions of saturated $NaHCO_3$, dried (Na_2SO_4), filtered, and concentrated. Column chromatography (4% CH_3OH/CH_2Cl_2) followed by preparative HPLC (30:70 hexanes:ethanol, 10 μ 100 Å (R,R) Whelk-O, 25 cm × 21.1 mm ID) provided 0.11 g of the ketone **15** as a white powder. ^{1}H NMR (400 MHz, $CDCl_3$): δ 8.67 (d, J = 4.93 Hz, 1H), 7.98 (m, 2H), 7.94 (m, 1H), 7.89 (d, J = 8.23 Hz, 1H), 7.84 (m, 3H), 7.77 (m, 1H), 7.72 (s, 1H), 7.53 (m, 2H), 7.46 (m, 4H), 7.40 (m, 1H), 7.29 (m, 1H), 6.84 (d, J = 6.13 Hz, 1H), 6.65 (d, J = 7.80 Hz, 1H), 5.10 (m, 2H), 4.61 (dd, J = 19.1, 1.22 Hz, 1H), 4.11 (d,

J = 14.8 Hz, 1H), 3.73 (d, J = 19.0 Hz, 1H), 3.42 (m, 2H), 2.64 (m, 1H), 2.24 (m, 1H), 2.16 (m, 1H), 1.84 (m, 1H), 1.38 (m, 1H). ^{13}C NMR (125.77 MHz, $CDCl_3$): δ 205.1, 169.8, 169.2, 157.2, 150.2, 138.2, 134.2, 134.0, 133.8, 132.6, 130.9, 130.0, 128.7, 128.2, 128.1, 127.7, 127.6 (2), 127.2 (2), 127.0, 126.4, 126.3, 125.9, 125.2, 125.2, 124.6, 122.4, 58.5, 57.8, 55.0, 51.3, 39.0, 31.8, 28.3. MS (ES) 621.0 $(M + H)^+$. Elemental analysis ($C_{35}H_{32}N_4O_5S \cdot 0.5H_2O$) C, H, N.

{(*S*)-1-[(3*R*,4*S*)-3-Hydroxy-1-(pyridine-2-sulfonyl)azepan-4-ylcarbamoyl]-2-naphthylen-2-yl-ethyl}carbamic Acid *tert*-Butyl Ester (18). To a solution of amino alcohol **17** (0.065 g, 0.211 mmol), EDC (0.045 g, 0.235 mmol), HOBt (0.031 g, 0.229 mmol), and Boc-L-naphthylalanine (0.067 g, 0.212 mmol) in CH_2Cl_2 (2.4 mL) was added triethylamine (0.12 mL, 0.861 mmol). The reaction was stirred at room temperature under argon for 4 days. After concentration of the reaction mixture in vacuo, column chromatography (2−3% CH_3OH/CH_2Cl_2) produced 0.091 g (76% yield) of **18** as a white solid. ^{1}H NMR ($CDCl_3$, 400 MHz): δ 8.62 (d, J = 4.24 Hz, 1H), 8.00 (d, J = 7.77 Hz, 1H), 7.93 (t, J = 7.46 Hz, 1H), 7.79 (m, 3H), 7.65 (s, 1H), 7.52 (dd, J = 7.38, 4.88 Hz, 1H), 7.46 (m, 2H), 7.36 (d, H = 7.97 Hz, 1H), 6.51 (d, J = 7.15 Hz, 1H), 5.07 (m, 1H), 4.41 (m, 1H), 4.05 (m, 1H), 3.77 (m, 1H), 3.56 (m, 1H), 3.35−3.16 (m, 5H), 1.84 (m, 1H), 1.67 (m, 2H), 1.57 (m, 1H), 1.49 (s, 9H). ^{13}C NMR (125.77 MHz, $CDCl_3$): δ 170.3, 157.0, 149.6, 138.5, 134.1, 133.4, 132.4, 128.4, 128.0, 127.7, 127.5, 127.3, 126.9, 126.2, 125.7, 123.3, 69.3, 55.8, 54.6, 48.4, 47.9, 38.9, 28.2, 26.4, 24.0. MS (ESI) 569.4 $(M + H)^+$.

Naphthalene-2-carboxylic Acid {(*S*)-2-Naphthalen-2-yl-1-[(*S*)-3-oxo-1-(pyridine-2-sulfonyl)azepan-4-ylcarbamoyl]ethyl}amide (15). To a solution of **18** (0.08 g, 0.14 mmol) in CH_3OH (1.8 mL) was added HCl (0.37 mL, 4.0N in dioxane). This mixture was maintained under argon for 19 h whereupon it was concentrated in vacuo and dried azeotropically three times with toluene. The crude product was carried to the next step with no further purification. To a solution of the amine hydrochloride (0.071 g, 0.141 mmol) in CH_2Cl_2 were added triethylamine (0.08 mL, 0.574 mmol), EDC (0.031 g, 0.162 mmol), HOBt (0.022 g, 0.163 mmol), and 1-naphthoic acid (0.025 g, 0.145 mmol) in CH_2Cl_2. This mixture was maintained at room temperature for 24 h whereupon it was concentrated in vacuo. Column chromatography (2%-5% CH_3OH/CH_2Cl_2) produced 0.050 g (57% yield over two steps) of the intermediate alcohol as a white solid. ^{1}H NMR ($CDCl_3$, 400 MHz): δ 8.64 (d, J = 4.23 Hz, 1H), 8.03 (d, J = 7.82 Hz, 1H), 7.95 (m, 2H), 7.88 (d, J = 8.17 Hz, 1H), 7.85 (m, 3H), 7.74 (m, 2H), 7.51 (m, 2H), 7.46 (m, 5H), 7.38 (m, 1H), 7.26 (m, 1H), 6.72 (d, J = 8.13 Hz, 1H), 6.67 (d, J = 7.81 Hz, 1H), 5.08 (dd, J = 14.8, 7.32 Hz, 1H), 4.14 (dd, J = 15.5, 5.04 Hz, 1H), 3.83 (m, 1H), 3.64 (m, 1H), 3.40 (m, 4H), 3.25 (d, J = 15.5 Hz, 1H), 1.87 (m, 1H), 1.78 (m, 1H), 1.62 (m, 2H). ^{13}C NMR (125.77 MHz, $CDCl_3$): δ 169.8, 169.2, 156.9, 149.6, 138.5, 133.6, 132.5, 130.8, 129.9, 128.6, 128.2, 127.7, 127.5, 127.3, 127.1, 127.0, 126.4, 126.3, 125.8, 125.2, 124.6, 123.4, 69.4, 55.0, 54.8, 48.2, 47.8, 39.0, 26.5, 24.0. MS(ESI) 623.4 $(M + H)^+$. To a solution of the alcohol (0.040 g, 0.064 mmol) in CH_2Cl_2 (1.0 mL) was added Dess−Martin periodinane (0.044 g, 0.104 mmol). This mixture was maintained at room temperature for 45 min whereupon it was diluted with CH_2Cl_2 and washed with 10% $Na_2S_2O_3$ (aqueous) and two times with saturated $NaHCO_3$. The combined $NaHCO_3$ layers were back extracted with CH_2Cl_2, and the combined organic layers were dried over Na_2SO_4, filtered, and concentrated. Column chromatography (1:1 hexanes:ethyl acetate) of the residue yielded 0.036 g (90%) of **15** as a white solid.

Supporting Information Available: Elemental analysis and HPLC data. This material is available free of charge via the Internet at http://pubs.acs.org.

References

(1) (a) Venter, C. J.; et al. The sequence of the human genome. *Science* **2001**, *291*, 1304−1351. (b) Lander, E. S.; et al. Initial sequencing and analysis of the human genome. *Nature* **2001**, *409*, 860−921. (c) Brömme, D.; Kaleta. Thiol-depedent cathepsins: Pathophysiological implications and recent advances in inhibitor design. *J. Curr. Pharm. Des.* **2002**, *8*, 1639−1658.

(2) (a) Marquis, R. W. Inhibition of the cystiene protease cathepsin K. *Ann. Rep. Med. Chem*. **2004**, *39*, 79−98. (b) Deaton, D. N.; Kumar, S. *Prog. Med. Chem.* **2004**, *42*, 245−375. (c) Veber, D. F.; Drake, F. H.; Gowen, M. The new partnership of genomics and chemistry for accelerated drug discovery. *Curr. Opin. Chem. Biol.* **1997**, *1*, 151−156.

(3) Marquis, R. W.; Ru, Y.; LoCastro, S. M.; Zeng, J.; Yamashita, D. S.; Oh, H.-J.; Erhard, K. E.; Davis, L. D.; Tomaszek, T. A.; Tew, D.; Salyers, K.; Proksch, J.; Ward, K.; Smith, B.; Levy, M.; Cummings, M. D.; Haltiwanger, R. C.; Trescher, G.; Wang, B.; Hemling, M. E.; Quinn, C. J.; Cheng, H.-Y.; Lin, F.; Smith, W. W.; Janson, C. A.; Zhao, B.; McQueney, M. S.; D'Alessio, K.; Lee, C.-P.; Marzulli, A.; Dodds, R. A.; Blake, S.; Hwang, S.-M.; James, I. E.; Gress, C. J.; Bradley, B. R.; Lark, M. W.; Gowen, M.; Veber, D. F. Azepanone-based inhibitors of human and rat cathepsin K. *J. Med. Chem*. **2001**, *44*, 1380−1395.

(4) (a) Turk, B.; Turk, D.; Turk, V. Lysosomal cysteine proteases: More than scavengers. *Biochim. Biophys. Acta* **2000**, *1477*, 98−11. (b) Kirschke, H.; Langner, J.; Wiederranders, B.; Ansorge, S.; Bohley, P.; Cathepsin, L. A new proteinase from rat-liver lysosomes. *Eur. J. Biochem*. **1977**, *74*, 293−301.

(5) Nakagawa, T.; Roth, W.; Wong, P.; Nelson, A.; Farr, A.; Deussing, J.; Villadangos, J. A.; Ploegh, H.; Peters, C.; Rudensky, A. Y. Cathesin, L. Critical role in Ii degradation and CD4 T cell selection in the thymus. *Science* **1998**, *280*, 450−453.

(6) Robker, R. L.; Russell, D. L.; Espey, L. L.; Lyndon, J. P.; O'Malley, B. W.; Richards, J. S. Progesterone-regulated genes in the ovulation process: ADAMTS-1 and cathepsin L proteases. *Proc. Natl. Acad. Sci*. **2000**, *97*, 4689−4694.

(7) Kirschke, H.; Eerola, R.; Hopsu-Havu, V. K.; Brömme, D.; Vuorio, E. Antisense RNA inhibition of cathepsin L expression reduces tumorigenicity of malignant cells. *Eur. J. Cancer* **2000**, *36*, 787−795 and references therein.

(8) Iwata, Y.; Mort, J. S.; Tateishi, H.; Lee, E. R. Macrophage cathepsin L, a factor in the erosion of subchondral bone in rheumatoid arthritis. *Arthritis Rheum.* **1997**, *40*, 499−509.

(9) (a) Furuyama, N.; Fujisawa, Y. Distinct roles of cathepsin K and cathepsin L in osteoclastic bone resorption. *Endocr. Res.* **2000**, *26*, 189−204. (b) Kakegawa, H.; Nikawa, T.; Kamioka, H.; Sumitani, K.; Kawata, T.; Drobnic-Kosorok, M.; Lenarcic, B.; Turk, V.; Katunuma, N. Participation of cathepsin L on bone resorption. *FEBS Lett.* **1993**, *321*, 247−250.

(10) Benavides, F.; Venables, A.; Klug, H. P.; Glasscock, E.; Rudensky, A.; Gomez, M.; Palenzuela, N. M.; Guenet, J.-L.; Richie, E. R.; Conti, C. J. The CD4-T cell-deficient mouse mutation nackt (nkt) involves a deletion in the cathepsin L (Ctsl) gene. *Immunogenetics* **2001**, *53*, 233−242.

(11) Potts, W.; Bowyer, J.; Jones, H.; Tucker, D.; Freemont, A. J.; Millest, A.; Martin, C.; Vernon, W.; Neerunjun, D.; Slynn, G.; Harper, F.; Maciewicz, R. Cathepsin-L deficient mice exhibit abnormal skin and bone development and show increased resistance to osteoporosis following ovariectomy. *Int. J. Exp. Pathol.* **2004**, *85*, 85−96.

(12) (a) Woo, J.-T.; Yamaguchi, K.; Hayami, T.; Kobori, T.; Sigeizumi, S.; Sugimoto, K.; Kondo, K.; Tsuji, T.; Ohba, Y.; Tagami, K.; Sumitani, K. Suppresive effect of N-(benzyloxycarbonyl)-L-phenylalanyl-L-tyrosinal on bone resorption in vitro and in vivo. *Eur. J. Pharmacol.* **1996**, *300*, 131−135. (b) Millest, A. J.; Breen, S. A.; Loveday, B. E.; Clarkson, P. N.; Sipson, C. A.; Waterton, J. C.; Johnstone, D. Effects of an inhibitor of cathepsin L on bone resorption in thyroparathroidectomized and ovariectomized rats. *Bone* **1997**, *20*, 465−471.

(13) Yasuma, T.; Oi, S.; Choh, N.; Nomura, T.; Furuyama, N.; Nishimura, A.; Fujisawa, Y.; Sohda, T. Synthesis of peptide aldehyde derivatives as selective inhibitors of human cathepsin L and their inhibitory effect on bone resorption. *J. Med. Chem*. **1998**, *41*, 4301−4308.

(14) Stroup, G. B.; Lark, M. L.; Veber, D. F.; Bhattacharyya, A.; Blake, S.; Dare, L. C.; Erhard, K. F.; Hoffmann, S. J.; James, I. E.; Marquis, R. W.; Ru, Y.; Vasko-Moser, J. A.; Smith, B. R.; Tomaszek, T. A.; Gowen, M. Potent and selective inhibition of human cathepsin K leads to inhibition of bone resorption in vivo in a nonhuman primate. *J. Bone Miner. Res*. **2001**, *16*, 1739−1746.

(15) (a) Mottram, J. C.; Brooks, D. R.; Coombs, G. H. Roles of cysteine proteinases of trypanosomes and Leishmania in host-parasite interactions. *Curr. Opin. Microbiol*. **1998**, *1*, 455. (b) McKerrow, J. H.; McGrath, M. E.; Engel, J. C. The cysteine protease of Trypanasoma cruzi as a model for antiparasitic drug design. *Parasitol. Today* **1995**, *11*, 279−282.

(16) Trout, R. E. L.; Marquis, R. W. Asymmetric synthesis of a potent azepanone-based inhibitor of the cysteine protease cathepsin K. *Tetrahedron Lett.* **2005**, *46*, 2799−2801.
(17) James, I. E.; Lark, M. W.; Zembryki, D.; Lee-Rykaczewski, E. V.; Hwang, S.-M.; Tomaszek, T. A.; Belfiore, P.; Gowen, M. Development and characterization of a human in vitro resorption assay: Demonstration of utility using novel antiresorptive agents. *J. Bone Miner. Res.* **1999**, *14*, 1562−1569.
(18) Dodds, R. A.; James, I. E.; Rieman, D.; Hwang, S.-M.; Ahern, R.; Conner, J. R.; Thompson, S.; Veber, D.; Drake, F. H.; Holmes, S.; Lark, M. W.; Gowen, M. Human osteoclast cathepsin K is processed intracellularly prior to attachment and bone resorption. *J. Bone Miner. Res.*, **2001**, *16*, 478−486.
(19) Definitive data for the presence of a similar intramolecular hydrogen bond was observed in the X-ray crystal structure of the closely related P3 quinoline-8-carboxamide **16**.

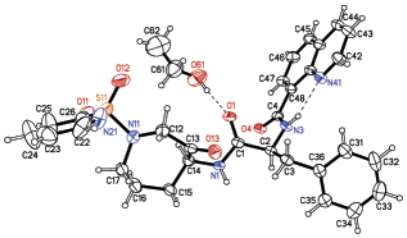

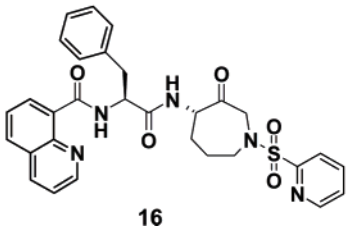

16

(20) Marquis, R. W.; Ru, Y.; Zeng, J.; Trout, R. E. L.; LoCastro, S. M.; Gribble, A. D.; Witherington, J.; Fenwick, A. E.; Garnier, B.; Tomaszek, T. A.; Tew, D.; Hemling, M. E.; Quinn, C. J.; Smith, W. W.; Zhao, B.; McQueney, M. S.; Janson, C. A.; D'Alessio, K.; Veber, D. F. Cyclic ketone inhibitors of the cysteine protease cathepsin K. *J. Med. Chem.* **2001**, *44*, 725−736.
(21) Within these series, N-methylation of this amide N−H moiety resulted in significant losses of potency vs the cathepsins studied.
(22) (a) Coulombe, R.; Grochulski, P.; Sivaraman, J.; Menard, R.; Mort, J. S.; Cygler, M. Structure of human procathepsin L reveals the molecular basis of inhibition of the prosegment. *EMBO J.* **1996**, *15*, 5492−5503. (b) Groves, M. R.; Coulombe, R.; Jenkins, J.; Cygler, M. Structural basis for specificity of papain-like cysteine protease proregions toward their cognate enzymes proteins. *Struct., Funct., Genet.* **1998**, *32*, 504.
(23) In the absence of X-ray cocrystal data of either **6** or **7** within the active site of cathepsin L, we are assuming that these inhibitors orient themselves on the unprimed side of the active site in a similar fashion as inhibitor **1** within the active site of cathepsin K. Additionally, we anticipate that the active site cysteine residue has added to the sterically more conjested *re* face of the ketone carbonyl moiety as was observed in the X-ray cocrystal structures of several azapanone-based inhibitors bound within the active site of cathepsin K.
(24) Brömme, D.; Klaus, J. L.; Okamoto, K.; Rasnick, D.; Palmer, J. T. Peptidyl vinyl sulphones: A new class of potent and selective cysteine protease inhibitors. *Biochem. J.* **1996**, *315*, 85−89.
(25) (a) McGrath, M. E.; Eakin, A. E.; Barnes, M. G.; Brömme, D. Crystal structure of human cathepsin K complexed with a potent inhibitor. *Nat. Struct. Biol.* **1997**, *5*, 104−109. (b) Zhao, B.; Janson, C. A.; Amegadzie, B. Y.; D'Alessio, K.; Griffin, C.; Hanning, C. R.; Jones, C.; Kurdyla, J.; McQueney, M. S.; Qui, X.; Smith, W. W.; Abdel-Meguid, S. S.. Crystal structure of human osteoclast cathepsin K complex with E-64. *Nat. Struct. Biol.* **1997**, *4*, 109−111.
(26) James, I. E.; Marquis, R. W.; Blake, S. M.; Hwang, S. M.; Gress, C. J.; Ru, Y.; Zembryki, D.; Yamashita, D. S.; McQueney, M. S.; Tomaszek, T. A.; Oh, H.-J.; Gowen, M.; Veber, D. F.; Lark, M. W. Potent and selective inhibitors of cathepsin L do not inhibit human osteoclast resorption in vitro. *J. Biol. Chem.* **2001**, *276*, 11507−11511.
(27) A correction to ref 26 has been published. James, I. E.; Marquis, R. W.; Blake, S. M.; Hwang, S. M.; Gress, C. J.; Ru, Y.; Zembryki, D.; Yamashita, D. S.; McQueney, M. S.; Tomaszek, T. A.; Oh, H.-J.; Gowen, M.; Veber, D. F.; Lark, M. W. Potent and selective inhibitors of cathepsin L do not inhibit human osteoclast resorption in vitro. *J. Biol. Chem.* **2003**, *278*, 32484.
(28) Our analysis of the selectivities of the potent cathepsin L peptide aldehyde inhibitors **16** and **17**, reported in refs 12a and 13, respectively, revealed that these analogues were equally potent inhibitors of both cathepsins K and S in addition to the potent inhibition of cathepsin L. These results, which were not reported in the referenced accounts, suggests that the conclusions regarding the mode by which these inhibitors may have elicited their antiresorptive effect were ambiguous.

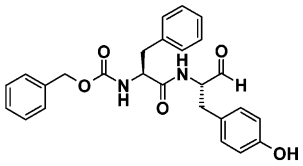

16

Cat L $K_{i,app}$ = 0.47 nM
Cat K $K_{i,app}$ = 0.74 nM
Cat S $K_{i,app}$ = 0.26 nM

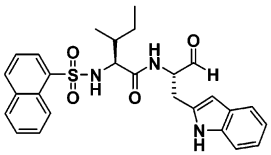

17

Cat L $K_{i,app}$ = 0.87 nM
Cat K $K_{i,app}$ = 2.0 nM
Cat S $K_{i,app}$ = 0.56 nM

JM0502079